Direct Manipulation of Malaria Parasites with Optical Tweezers Reveals Distinct Functions of Plasmodium Surface Proteins

Stephan Hegge,[†,||] Kai Uhrig,[†,‡,||] Martin Streichfuss,[‡] Gisela Kynast-Wolf,[§] Kai Matuschewski,[†,⊥] Joachim P. Spatz,[‡] and Friedrich Frischknecht[†,*]

[†]Parasitology, Department of Infectious Diseases, University of Heidelberg Medical School, Im Neuenheimer Feld 324, 69120 Heidelberg, Germany, [‡]Department of New Materials and Biosystems, Max Planck Institute for Metals Research, and Department of Biophysical Chemistry, University of Heidelberg, Heisenbergstr. 3, 70569 Stuttgart, Germany, [§]Institute for Public Health, University of Heidelberg Medical School, Im Neuenheimer Feld 324, 69120 Heidelberg, Germany, and [⊥]Parasitology Unit, Max Planck Institute for Infection Biology, Chariteplatz 1, Campus Charite Mitte, 10117 Berlin, Germany. [||]These authors contributed equally to this work.

During eukaryotic cell adhesion, external signals are transduced to the cytoskeleton at distinct adhesion sites *via* adhesion-mediating proteins such as integrins or cadherins. In turn, the strength of adhesion is frequently determined and modulated by the cytoskeleton that is linked to those adhesion-mediating proteins.[1,2] During motility, adhesion sites have to be assembled at the leading end while they need to be disassembled or ruptured at the trailing end.[3,4] Adhesion sites are held together by internal interactions between proteins (cohesion) that need to be stronger than the adhesive interactions of these proteins with molecules on the substrate.

The highly motile *Plasmodium* sporozoites are deposited in the skin of the host during the bite of a mosquito leading to the transmission of malaria.[5−7] Sporozoites migrate rapidly within the dermis, can enter blood vessels, and migrate again on the liver endothelium and parenchyma before entering a hepatocyte for replication.[8,9] Adhesion is a prerequisite for motility, which in turn is essential for tissue penetration and host cell invasion. Sporozoite motility is regulated by the dynamic turnover of distinct adhesion sites and employs an actin−yosin-based gliding machinery, which is linked to the substrate *via* the transmembrane proteins of the TRAP (thrombospondin-related anonymous protein) family.[10−13]

Adhesion of sporozoites is likely mediated by proteins on the sporozoite surface, like circumsporozoite protein (CSP), which is the major surface protein of the sporozoite,[14] members of the TRAP family,[12,15] MAEBL[16] and *Plasmodium* cysteine repeat modular proteins (PCRMP) 1 and 2.[17] Sporozoites adhere to a large variety of substrates including polyacrylamide, gold, and carbon surfaces.[13,18,19] We recently established that adhesion of sporozoites to a 2D surface occurs in a multistep sequence with distinct adhesion intermediates.[20] Sporozoites attach at either the front or rear end, then adhere with the other end and finally with the central part before starting to move. While moving, sporozoites can be attached

ABSTRACT

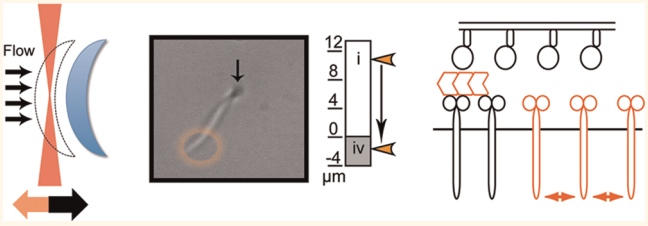

Plasmodium sporozoite motility is essential for establishing malaria infections. It depends on initial adhesion to a substrate as well as the continuous turnover of discrete adhesion sites. Adhesion and motility are mediated by a dynamic actin cytoskeleton and surface proteins. The mode of adhesion formation and the integration of adhesion forces into fast and continuous forward locomotion remain largely unknown. Here, we use optical tweezers to directly trap individual parasites and probe adhesion formation. We find that sporozoites lacking the surface proteins TRAP and S6 display distinct defects in initial adhesion; *trap(-)* sporozoites adhere preferentially with their front end, while *s6(-)* sporozoites show no such preference. The cohesive strength of the initial adhesion site is differently affected by actin filament depolymerization at distinct adhesion sites along the parasite for *trap(-)* and *s6(-)* sporozoites. These spatial differences between TRAP and S6 in their functional interaction with actin filaments show that these proteins have nonredundant roles during adhesion and motility. We suggest that complex protein−protein interactions and signaling events govern the regulation of parasite gliding at different sites along the parasite. Investigating how these events are coordinated will be essential for our understanding of sporozoite gliding motility, which is crucial for malaria infection. Laser tweezers will be a valuable part of the toolset.

KEYWORDS: optical traps · apicomplexa · sporozoites · gliding motility · adhesin · cohesion

* Address correspondence to freddy.frischknecht@med.uni-heidelberg.de.

Received for review September 20, 2011 and accepted May 8, 2012.

Published online May 08, 2012
10.1021/nn203616u

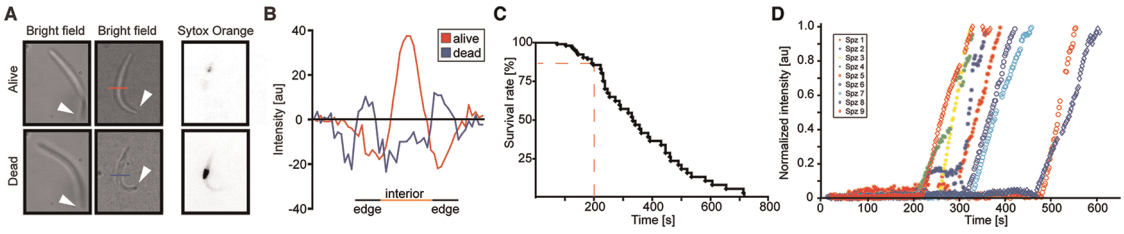

Figure 1. Plasmodium sporozoites survive trapping by optical tweezers. (A) Examples of visual identification of live and dead sporozoites. Living sporozoites (top panels) are defined by a clear contrast between parasite edges and the parasite interior in bright field and a faint Sytox Orange signal (signal is inverted for better visualization). After prolonged laser exposure (bottom panels), sporozoites show altered shapes that hardly silhouette against the background, display a marmoreal interior, or show an otherwise altered contrast. Invariably dead sporozoites show a strong nuclear Sytox Orange signal. Sytox Orange is a nuclear stain and thus also allows determining the polarity of the parasites (arrowheads point to front ends). The red and blue lines indicate the position along which the intensity profiles as presented in (B) were taken. (B) Intensity profiles of the sporozoite shown in (A). The intensity plots correspond to the cross sections as indicated in (A). Living parasites show high intensity amplitudes, indicating good contrast, whereas dead sporozoites mostly do not and show a variable degree of weaker contrast. (C) Survival curve of sporozoites trapped with a laser power of 100 mW at $t = 0$ s and held inside the focus of the laser until they were dead; 85% of probed sporozoites survived the first 200 s (red dashed lines). A total of 106 parasites (48 death events, 58 censored subjects at $t = 200$ s) were tested within 8 independent experiments. (D) Increase of nuclear (5 μM Sytox Orange) fluorescent signal of 9 immobile salivary gland sporozoites continuously exposed to 100 mW laser power of the optical trap. The sharp increase of the fluorescence intensity indicates the moment of membrane rupture, which appeared at 310 $\pm$ 102 s, similar to the 50% death time in (C). Gaps of several seconds appear when the microscope was switched to bright-field mode and then back to fluorescence mode.

with just one end and the central part of the parasite.[13,20] It was also shown that TRAP and S6 (also named TREP and UOS3) are involved in the overall adhesive capacity of sporozoites, while the TRAP-like protein (TLP) is needed for stable adhesion during motility.[20] In addition to its role in adhesion, TRAP appears to play an unidentified role in de-adhesion, as parasites that lack TRAP but do undergo initial adhesion cannot dissociate this first adhesion site from the substrate anymore, a prerequisite for productive motility.[13] Considering the occurrence of distinct adhesion and de-adhesion steps and the number of proteins present on the sporozoite surface, we hypothesize that these proteins play distinct roles in the different steps necessary for adhesion and motility.

Sporozoites form in cysts at the mosquito midgut wall, enter the hemolymph and finally the salivary glands from where they are ejected during a mosquito bite. The capacity of sporozoites to glide, like their capacity to adhere to a substrate, is more pronounced in sporozoites isolated from salivary glands than in sporozoites isolated from the hemolymph or midgut.[20] Several proteins have been implicated in either mediating sporozoite gliding, salivary gland invasion, or both. Sporozoites lacking MAEBL and PCRMP appear to glide normally but fail to invade salivary glands.[16,17] Parasites lacking TRAP cannot glide productively and fail to invade salivary glands,[10,13] while parasites lacking S6 can still enter into salivary glands in reduced numbers and also display weak motility.[21] Finally, sporozoites lacking TLP enter into salivary glands but show only a subtle reduction in gliding.[20,22] Taken together, this provides further evidence that proteins involved in adhesion also play a role in parasite motility. How they achieve this role and whether they act through cytoplasmic actin filaments remains unclear. To mark a further challenge, *Plasmodium* actin filaments appear to be short[23−25] and have so far not been visualized in intact sporozoites.[26]

Here we trap and manipulate *Plasmodium berghei* sporozoites with optical tweezers to gain quantitative insights into the molecular basis of sporozoite adhesion. Optical tweezers are versatile tools to manipulate microscopic objects and apply forces on specimens that are trapped in the focus of a laser beam. Experiments using optical tweezers have been performed to study single bacteria and viruses[27] as well as *Plasmodium falciparum* infected erythrocytes.[28,29] Here we probed sporozoites in both the presence and absence of the TRAP family proteins TRAP and S6 as well as actin filaments. As *trap(-)* parasites do not enter into salivary glands, we examined exclusively parasites isolated from the hemolymph of the mosquito. This allowed us to uncover specific and redundant roles for TRAP and S6 during the initial step of sporozoite adhesion.

RESULTS

Plasmodium Sporozoites Can Be Trapped by Optical Tweezers. Hemolymph-derived *Plasmodium berghei* sporozoites were isolated from infected mosquitoes 16 days post-infection (dpi), placed in RPMI containing 3% bovine serum albumin (BSA) and the DNA stain Sytox Orange [5 μM] in a tailored imaging chamber, and allowed to adhere. As determined previously, hemolymph sporozoites followed the same stepwise adhesion pattern described for salivary-gland-derived sporozoites. However, a proportion (~20%) of hemolymph sporozoites showed an active movement, termed patch gliding.[13,20,30] During patch gliding, a parasite is stuck to the substrate with a small adhesion site and, instead

of continuing adhesion, continuously moves back-and-forth over this adhesion site.

Since sporozoites possess a refractive index higher than the surrounding medium, we were able to trap sporozoites in the focus of the optical tweezers. To facilitate capturing the otherwise rapidly moving sporozoites, we first applied 2 μM cytochalasin D to the sporozoites. Addition of this actin inhibitor abolished gliding locomotion.[30] Importantly, sporozoites stayed attached to the substrate under this drug concentration. This allowed us to determine the conditions for manipulating the parasites. Optical tweezers for biological applications are usually designed to use wavelengths in near-infrared since this spectral window is known to show very little absorption in aqueous samples from biological objects.[27,31,32] However, the high intensity of the incident light can heat up cells[33] and cause photodamage, which can be harmful for the cell. Thus, we first investigated the influence of the laser tweezers on the survival of sporozoites (Figure 1). Living *P. berghei* sporozoites are elongated cells with a crescent shape (Figure 1A). When using bright-field microscopy, sporozoites in focus showed a strong contrast at the edges and a bright interior (Figure 1A,B). In contrast, dead sporozoites showed an aberrant shape and structure: the interior appeared marmoreal, and the sharp contrast at the edges was diminished (Figure 1A,B). The rupture of the parasite membrane and thus the presumed parasite death could additionally be detected by the increased nuclear staining of the non-membrane-permeable dye Sytox Orange (Figure 1A,B). Clear differences between living and dead sporozoites in the fluorescence images thus allowed the determination of sporozoite viability in the laser traps (Figure 1A). Under continuous trapping, more than 85% of over 100 probed sporozoites survived the first 200 s inside a 100 mW laser trap (Figure 1C,D). Therefore, we performed experiments only within this time span.

Force Calibration of Trapped Sporozoites. To access reliable values for the forces exerted by the optical tweezers on an object, we next calibrated our setup.[34] However, calibrating the spring constant for a trap holding an asymmetric sporozoite is not as straightforward as for spherical objects like beads.[35] Since sporozoites are far bigger than the focus of the laser, the laser can be moved in the volume of the object along the axis for some micrometers without causing significant forces. Therefore, simple calculations of the exerted forces based on Brownian motion do not lead to correct results. We thus used a calibration methodology based on hydrodynamic friction forces to determine the maximum trapping forces at which the objects escape the trap.[36] To this end, the microscope stage was moved at increasing velocities until the hydrodynamic friction of the medium overcame the trapping strength of the laser and the object was pushed out of the trap (Figure 2A).

The calculation of the friction force acting on an object depends on its shape and volume. In a first approximation, we considered the crescent-shaped sporozoites as prolate spheroids with $a = 6$ μm and $b = 0.5$ μm, which corresponds to estimates of sporozoite dimensions from electron microscopy studies[37,38] (Figure 2B). For this surrogate sporozoite, we obtained a Perrin factor of $S = 1.64$ (for detailed description to calculate S, see Supporting Information Text 1).

As the sporozoite is not a rigid object, it can bend and adjust its orientation to minimize friction. Thus, the calculated forces provide an upper limit of the potential trapping force F_{max} for prolate ellipsoids, whereas the calculations for an isovoluminous sphere represent the minimum forces F_{min} acting on a sporozoite in a hydrodynamic flow. The real shape and thus the real friction force acting on the sporozoite F_{real} is considered to lie between F_{max} and F_{min} for a given laser power of the trap (Figure 2B). To estimate F_{real}, escape velocities were measured for different laser powers and the respective forces for a sphere and spheroid were calculated (Figure 2C). For 100 mW trapping power, the minimal force F_{Sphere} was determined by linear regression as 4.0 ± 0.9 pN and the upper limit $F_{Spheroid}$ as 6.6 ± 1.4 pN. For the maximum applied laser power of 450 mW, the respective values were $F_{Sphere} = 15.0 \pm 2.6$ pN and $F_{Spheroid} = 24.6 \pm 4.3$ pN. This calibration applies only on forces acting in the *xy*-plane and serves as the lowest estimate for forces acting in *z*-direction.

3D Manipulation of Plasmodium Sporozoites Using Optical Tweezers. We next tested whether sporozoites can be manipulated at various stages during the adhesion process. Capturing sporozoites permitted the induction of early adhesion (Figure 3). For instance, sporozoites that were attached with one end to the glass surface could be trapped on their free end, and by gently moving the microscope stage relative to the stationary laser focus, a force could be applied that led to a displacement of the sporozoite (Figure 3B). In this way, the free end could be moved horizontally or vertically (Figure 3B,C).

We first probed the rotational flexibility (or lateral cohesion; for definition, see Methods) of each sporozoite by trapping the free floating end of a single-end attached parasite and rotating it in *xy*-direction (Figure 3B,D). This showed that individual sporozoites differed substantially with rotation angles ranging from 0 to 360°, with each population of examined parasites showing a median of 360° (Figure 3D, Figure S2, and below). This finding indicates that F-actin does not contribute to rotatability and thereby lateral cohesion strength (Figure S2A). To further analyze the data, we pooled all cytochalasin-treated and nontreated *trap(-)* sporozoites as well as *s6(-)* parasites. No

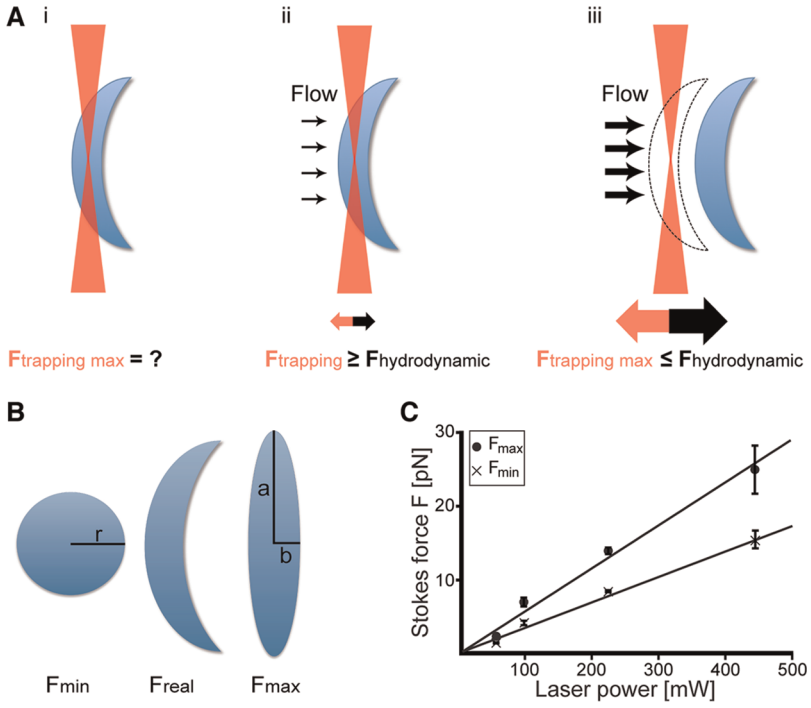

Figure 2. Calculating Stokes forces acting on sporozoites. (A) Scheme of force calibration for sporozoite experiments. A sporozoite is held in an optical trap (i). When a flow is applied, a hydrodynamic friction force acts on the parasite (ii). This force is proportional to the velocity of the flow. At a certain flow speed, the friction force exceeds the trapping force of the optical tweezers and the sporozoite is pushed out of the trap (iii). Estimating the friction factor and measuring the velocity of the flow allows the calculation of the escape force acting on the sporozoite. (B) Model for Perrin friction factors calculation for Plasmodium sporozoites. The geometry of a sporozoite (center) resembles an intermediate between a sphere (left) and a prolate spheroid (right) of identical volumes. Unlike sporozoites, prolate spheroides and spheres possess defined Perrin factors which serve to calculate an upper (F_{max}) and lower (F_{min}) holding force during a hydrodynamic friction based force calibration. (C) Escape forces for trapped sporozoites at different laser powers. A floating parasite was trapped at a given laser power. Next, a linear increase of stage velocity using a piezo-controlled stage led to increased hydrodynamic shear in consecutive experiments until the sporozoites were pushed out of the trap. The stage velocity translates into an upper (prolate spheroide, F_{max}) and lower (sphere, F_{min}) Stokes force, conferring the real holding force (sporozoite, F_{real}) between these values. Error bars represent SD of 7 sporozoites for every tested laser power.

significant difference (p value = 0.6) was found when comparing the rotatability of WT sporozoites in the presence of cytochalasin D (denoted as WT/F-actin(-)) with pooled *s6(-)* parasites. However, comparing WT/F-actin(-) sporozoites with those from pooled *trap(-)* parasites (p value = 0.07) indicates a possible influence of TRAP but not S6 on lateral cohesion of the primary adhesion site.

Subsequently, the trap was moved slightly underneath the glass surface, thereby forcing the free end of the sporozoite to contact the substrate (Figure 3C). Substrate contact is required for establishing a second adhesion side. Therefore, we anticipated that pulling and bringing the sporozoite in close contact with the surface may facilitate the formation of a second adhesion site (Figure 3E). However, sporozoites often failed to immediately establish a second adhesion. Therefore, the formation of a secondary adhesion by manipulation with the optical tweezers was attempted at several positions of the parasite. In case no secondary adhesion was formed within 200 s, the sporozoite was recorded as "failing to establish a secondary adhesion" (see below).

Adhesion State of Hemolymph Sporozoites. Sporozoites isolated from the mosquito hemolymph adhere substantially better than those isolated from midguts but less than salivary-gland-derived sporozoites.[20] We therefore examined the adhesion status of wild-type, *s6(-)*, and *trap(-)* sporozoites, which all produce similar numbers of hemocoel sporozoites (Figure 4A). As expected,[20] we found that knockout parasites generally adhered less well to the substrate than wild-type, thus corroborating critical roles for S6 and TRAP in establishing primary adhesion. Curiously, we found a significantly lower proportion of knock-out parasites establishing a second and third adhesion site, while the population forming single adhesion sites was similar, suggesting a role for both TRAP and S6 in the formation of secondary and tertiary adhesion sites (Figure 4A). The *s6(-)* sporozoites were still able to undergo full adhesion and a small number could resume gliding, while *trap(-)* sporozoites would not form more than one adhesion site (Figure 4A). Together, this revealed a difference in the capacity to adhere beyond the primary adhesion between *trap(-)* and *s6(-)* sporozoites suggesting a more pronounced role for TRAP

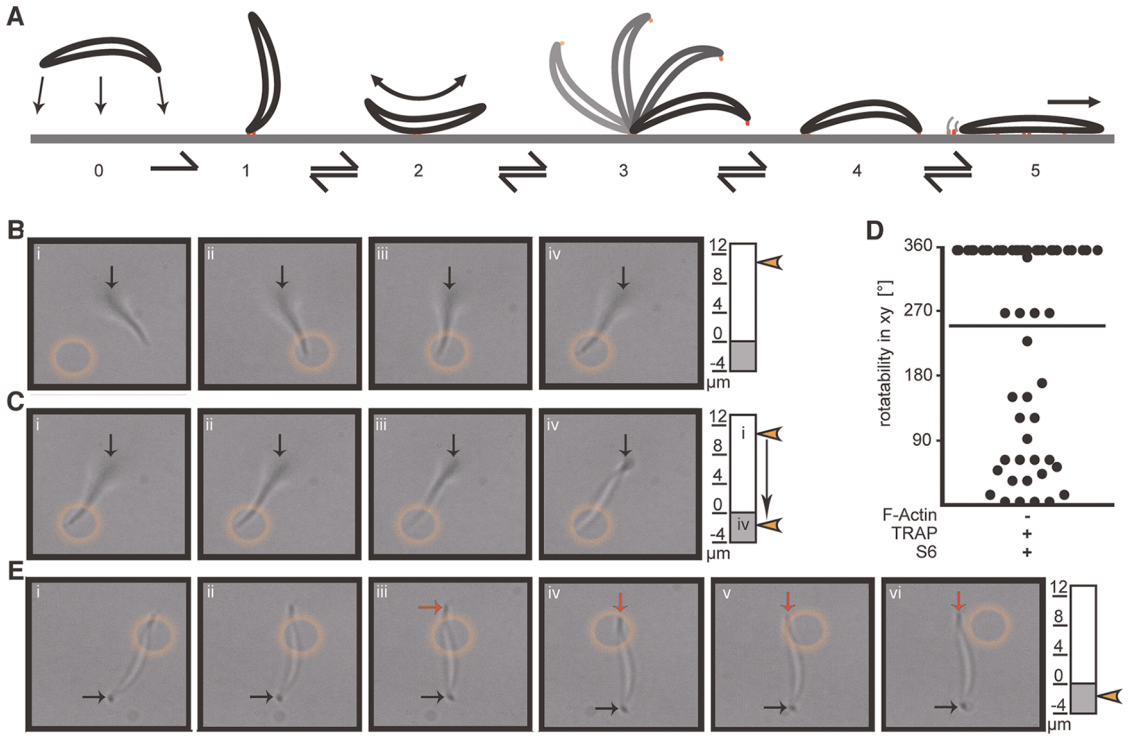

Figure 3. Manipulation of Plasmodium sporozoite adhesion with optical traps. (A) Typical adhesion and motility states of hemolymph sporozoites. (0) Floating parasite approaching a surface (gray line) can adhere at either the front or rear end or the central part (arrows). (1−3) Hemolymph sporozoites with one adhesion site (red lines) either attach without movement (1), perform pendulum-like gliding movements (patch gliding) over a single adhesion site (2), or wave actively with the free end (3). In all cases, the adhesion site remains constantly attached to the substratum. Waving is often followed by the formation of a second adhesion (4), which typically leads to a central third adhesion (5) and, finally, productive gliding. The "J" form of hemolymph parasites[6] allows identification of the front end, typically located at the curved end of the "J". (B) P. berghei sporozoite attached at one end (arrow, i) is captured by an optical trap (orange circle) at its free end (ii) and rotated in lateral direction (iii) by about 90° (iv) in the presence of cytochalasin D. The scheme (right) indicates the *z*-position of the focal plane, where the laser trap is located in the center of the orange circle. The orange arrow indicates that the focal plane at the laser trap is about 10 μm above the surface of the glass substrate. Thus, the adhesion site (arrow) is out of focus. (C) Focal plane of the laser is moved in *z*-direction from 10 μm above (i) to underneath the glass surface (iv). Since the free end of the parasite follows the trap (i−iv), it eventually touches and potentially adheres to the substrate. (D) Dot plot indicating the maximal lateral rotatability of wild-type sporozoites in the presence of cytochalasin D as shown in (B). The median is 360°, the average 252° (black line). For the rotatability of all mutants investigated in this study, see Figure S2. (E) Induction of a strong second adhesion site. Moving the sporozoite from (C) over the glass substrate while pulling it toward the substrate (i,ii) induces the formation of a second adhesion side at the free end trapped by the laser beam (iii, red arrow). Once firmly attached, the sporozoite no longer follows the movement of the optical trap (iv−vi) and the attachment can be considered "stable" and, therefore, counted as "second adhesion". Note that at the given laser power the adhesion site cannot be disrupted (iv−vi).

in the formation of a second adhesion site than for S6.

To dissect this difference, we next focused on where sporozoites established their first adhesion site. To this end, we investigated sporozoites in the presence (F-actin(-)) or absence (F-actin(+)) of the actin depolymerizing drug cytochalasin D. As reported,[20] WT/F-actin(+) parasites could attach at any side to the substrate and usually underwent rapid secondary and tertiary adhesion and started to glide. However, the speed of this process made it difficult to quantitatively analyze the exact distribution of where the parasite attached first. In contrast, WT/F-actin(-) parasites formed the first adhesion mainly at their front end (Figure 4B). The *trap(-)* sporozoites also showed a preference for adhesion with the front, irrespective of cytochalasin D. In contrast, *s6(-)* parasites showed a preference for adhesion with the front end only in the presence of cytochalasin D. Thus, in the absence of physiological actin dynamics or TRAP, the parasite adopts polarized adhesion, indicating that actin dynamics and TRAP are both important for appropriate adhesion formation along the sporozoite. This suggests that TRAP mediates adhesion in the presence of actin filaments at any site along the parasite. In contrast, S6 has either little influence on where sporozoites adhere or mediates adhesion at the front in an actin-independent way.

Initial Adhesion and Force Generator Strength. We next tested the strength of this initial adhesion. Under all tested conditions, this initial attachment was too strong to be ripped off with optical tweezers even when applying maximum laser power (450 mW) (not shown). Considering the calibrations in Figure 2, this indicates that the primary adhesion resists forces

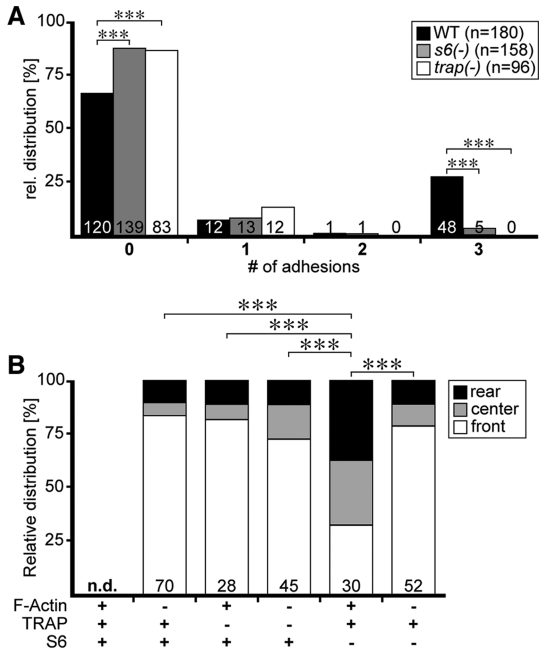

Figure 4. Distinct adhesion formation along the sporozoite surface. (A) Graph illustrating the distribution of adhesion points of hemolymph sporozoites: 0 adhesions, floating parasites; 1 adhesion, patch gliding, waving, or attached parasites with one free floating end; 2 adhesions, two adhesion points (rear-front; rear-center; front-center) and a clearly distinguishable unattached area; 3 adhesions, gliding sporozoites as well as parasites with no area prone to displacement by random motion. Every sporozoite was observed for 100 s. Only the maximal adhesion state was counted and considered for this graph in order to avoid double counting. (B) Position of the primary adhesion. Patch gliders are not considered, as they constantly change their position. Wild-type parasites were not tested (n.d.). Numbers in bars indicate the number of examined sporozoites. The *p* values refer to the comparison "adhesion at the front end" *versus* "adhesion not at the front end". Statistical differences are indicated by * ($p < 0.001$). "F-actin" indicates the absence (+) or presence (-) of cytochalasin D, "TRAP-" and "S6-" indicate the use of *trap(-)* or *S6(-)* sporozoites.**

of ≈25 pN (±20%) and that the lack of TRAP, S6, or actin filaments does not lead to a measurable destabilization of the first adhesion site once it is established.

Wild-type hemolymph sporozoites indeed readily form a first adhesion, which was either followed by patch gliding[13] or formation of a second adhesion, eventually leading to gliding (Figure 3A). As referred to earlier, in the absence of cytochalasin D, sporozoites could not be trapped when undergoing patch gliding (data not shown). This indicates that the motility machinery is capable of generating forces greater than 6.6 ± 1.4 pN over a single adhesion site in both directions. Curiously, however, patch gliding *trap(-)*/F-actin(+) as well as *s6(-)*/F-actin(+) sporozoites could readily be trapped, suggesting that the force transduction is considerably weaker in both mutant parasites than in the wild-type.

Cohesion of the Primary Adhesion Site Depends on S6. We next probed the linear cohesion of the primary adhesion site, that is, the capacity to resist forces applied along the sporozoite long axis. This could be achieved by pushing the sporozoite anchored at one end over the single adhesion site resulting in a *de facto* translocation of the adhesion patch along the sporozoite (Figure 5A). After a maximum of 200 s of probing, the outcome was classified as either "successful" or "not successful". This yielded a number of unexpected results. Upon addition of cytochalasin D, leading to disrupted actin filaments denoted as WT/F-actin(-), only 18% of wild-type parasites permit such pushing and pulling (Figure 5B). Under similar conditions, *trap(-)*/F-actin(-) sporozoites could be "pulled over" somewhat more frequently (33%, $p = 0.08$), while *s6(-)*/F-actin(-) sporozoites showed no difference. Unexpectedly, in the absence of cytochalasin D, 66% of *s6(-)*/F-actin(+) sporozoites could be pulled over the initial adhesion site (Figure 5B).

This finding prompted us to examine linear cohesion according to the position of the initial adhesion site (Figure 5C). In general, it was easiest to push parasites adhering with their central part. Monitoring *trap(-)* sporozoites with or without cytochalasin D showed no difference in the success rate for pushing sporozoites adhering with the front. In contrast, a significantly larger proportion ($p < 0.05$) of *trap(-)*/F-actin*(-)* parasites compared to *trap(-)*/F-actin(+) could be "pulled over" when adhering at their rear end (Figure 5C). In contrast to these findings but in good agreement with our previous results, *s6(-)*/F-actin(+) sporozoites could be pushed independently of the location of the initial adhesion site, and while disruption of actin filaments had no effect on the cohesive strength of rear end adhesions, actin filament disruption led to a significantly stronger ($p < 0.01$) cohesion of the adhesion site at the parasite front of *s6(-)*/F-actin(-) sporozoites (Figure 5C). Thus, the cohesive strengths of different adhesion sites depend on the distinct interplay of TRAP and S6 with actin filaments.

***s6(-)* Sporozoites Have a Higher Potential for Establishing a Second Adhesion.** Next, we attempted to induce a second adhesion as described in Figure 3, which was possible with 26% of wild-type parasites with disrupted actin filaments (Figure 6A). The success rate appeared higher for *s6(-)*/F-actin(+) compared to *s6(-)*/F-actin(-) ($p = 0.09$) and *trap(-)*/F-actin(-) ($p = 0.01$) or *trap(-)*/F-actin(+) ($p = 0.08$) parasites. This trend reflects the data from the "pull-over" experiments over the primary adhesion site (Figure 5B). Therefore, we assumed a correlation between the linear cohesion strength as determined from "pull-over" experiments and the potential to form a second adhesion. To test this, we retrospectively compared parasites that showed an initial and a second adhesion side at their tips and plotted the

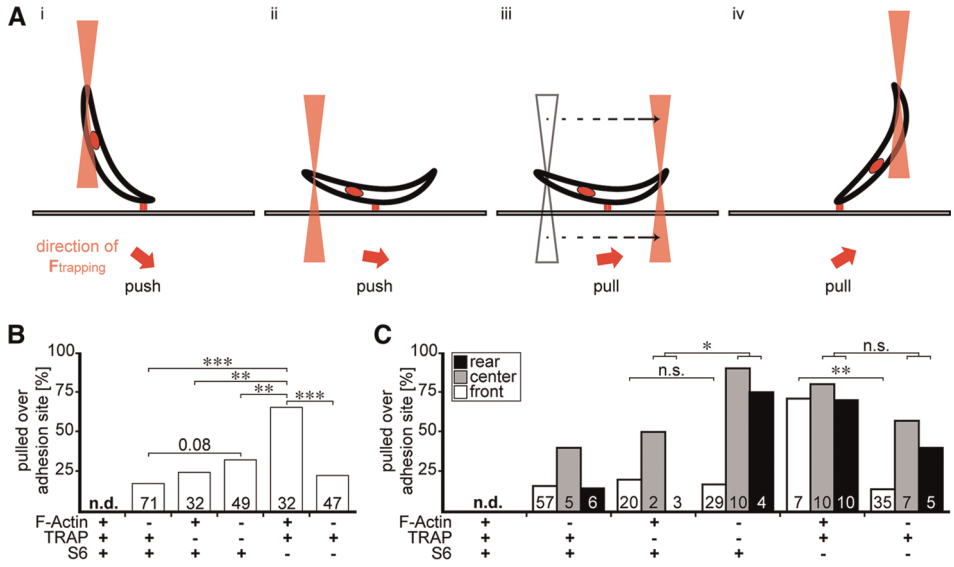

Figure 5. Cohesion differences of initial adhesion sites of *trap(-)* and *s6(-)* sporozoites. (A) Scheme of laser trap-mediated probing for linear cohesion. Adhesions (red lines), nucleus (red circle), substrate (gray bars), and the direction of the trapping force ($F_{trapping}$, arrow) are indicated. (i) Sporozoite with a primary adhesion site at the front is trapped with the laser tweezers at the free-floating rear end. Directed *xy* and *z* manipulation of the trap exerts a vectored force to the sporozoite, eventually pushing the trapped end toward the adhesion site. (ii) Trap pushes the parasite over its primary adhesion site, while the adhesion site maintains its position relative to the substrate. (iii) Position of the tweezers is changed from one (empty triangles) to the other side of the adhesion in order to swap from pushing to pulling the parasite. (iv) Tweezers pull the parasite until the rear end of the sporozoite is localized above the adhesion site. (B) Percentage of sporozoites that were successfully push-pulled over the first adhesion site. Wild-type parasites could not be determined since their movement was too strong to be trapped by 100 mW laser tweezers. (C) Quantification of the ability to push−pull sporozoites over their first adhesion site according to the initial position of the adhesion. Numbers in bars indicate the number of sporozoites examined for each experiment. The *p* values are indicated or shown as * ($p < 0.05$), ** ($p < 0.01$), or * ($p < 0.001$); n.s. not significant.**

successful attempts of "pulling over" prior to the establishment of a second adhesion site (Figure 6B). Only a small fraction (8%) of the WT/F-actin(-) parasites that ultimately formed two adhesions could be "pulled over", compared to 100% of *s6(-)*/F-actin(+) parasites (Figure 6B).

These results suggested that *s6(-)*/F-actin(+) parasites can establish more induced second adhesion sides. This might be due to an opportunity to use the apical, possibly more adhesive end (Figure S2B) for forming both the initial as well as the second adhesion site. In order to test this, we only examined sporozoites with a primary adhesion side at the front end on their ability to form a second adhesion with consideration to which end of the parasite forms the second adhesion (Figure 6C). Indeed, we found that in contrast to all other conditions the majority of *s6(-)*/F-actin(+) but hardly any *s6(-)*/F-actin(-) sporozoites used their apical end twice for forming cell−substrate adhesions (Figure 6C). This agrees with and explains the outcomes of the experiments in Figure 4B, Figure 5B,C, and Figure 6A,B. In conclusion, sporozoites employ distinct surface molecules to optimize establishment of initial and secondary adhesion sites.

DISCUSSION

Using cellular and biochemical adhesion assays, it has been shown that sporozoites adhere to various liver cells with their surface proteins circumsporozoite protein (CSP) and TRAP by binding proteoglycans.[39−41] These highly sulfated proteoglycans were identified as a trigger for target recognition.[39,42] However, the spatial and temporal details of the actual adhesion process remain largely unknown.[20] Here, we used genetically modified *Plasmodium berghei* parasites in combination with optical tweezers in order to establish an experimental routine to shed light on the biophysical and molecular processes occurring during distinct steps of the multistep adhesion process of sporozoites.

Laser Tweezers as New Tools To Study Malaria Parasites. Typically, optical tweezers deploy their full potential on spherical objects, thereby covering forces ranging from very few femto-Newtons up to several hundred pico-Newtons.[43,44] Provided the system allows trapping beads with optical tweezers and successfully attaching them to the biological sample of interest, the full range of forces can be used by varying the laser power. Force transducing polystyrene beads have been employed among others in combination with red blood cells[28,29] and to study the promastigote (flagellated) form of *Leishmania amazoniensis* parasites.[45] These studies probed elastic[28,29] or chemotactic[45] properties, and therefore, their additional attachment to beads was not influencing the tested parameters, as would be the case for probing adhesion events. As we could not afford blocking a potential

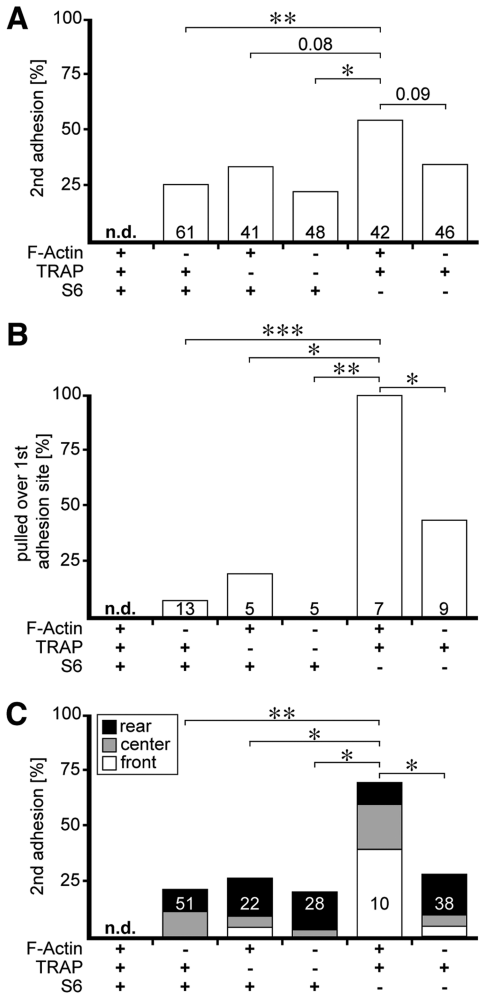

Figure 6. Differences in cohesion strength in *trap(-)* and *s6(-)* sporozoites leads to different rates of secondary adhesion. (A) Percentage of sporozoites with an induced second adhesion. (B) Percentage of parasites that were pulled over the first adhesion site and established a second adhesion. (C) Subpopulation of (A) to illustrate the percentage of induced second adhesions, provided the primary adhesion of the parasite was at the front. Note that only a certain fraction of sporozoites uses the front part for both adhesions (white area within the bars; see also Figure 5B). Gray and black areas within bars indicate adhesion to central and front part, respectively. Numbers in bars indicate the number of sporozoites examined for each experiment. The *p* values are indicated or shown as * ($p < 0.05$), ** ($p < 0.01$), or * ($p < 0.001$).**

adhesion site with a bead, we applied the tweezers directly on the sporozoite cell body. This approach avoided the blockage of an adhesion site on one hand; on the other hand, by deducting from the absorption effect of laser tweezers on red blood cells,[46] it ran the risk of heating up and thus killing the sporozoite (Figure 1). However, a moderate laser power (100 mW) could be used which allowed us to perform the experimental protocol within 1−3 min without killing parasites, although smaller damaging processes during the time of experimentation could not be completely excluded.

Force Calibration by Means of Hydrodynamic Shear Flow. We determined the actual holding force $\mathbf{F}_{trapping}$ by calibrating the optical tweezers with a method based on hydrodynamic friction forces (Figure 2).[36] The resulting holding forces showed a linear correlation to the applied laser power and ranged between 1.3 ± 0.2 and 24.6 ± 4.3 pN (Figure 2C). These forces are in the similar range as those applied *via* beads onto filopodia to measure their retraction,[47] although others have made use of the much higher forces that can be generated with beads serving as a force transducer.[43,48] This allowed us to determine that the initial adhesion withholds forces greater than 24.6 ± 4.3 pN as we hardly (<1%) managed to rip an attached sporozoite off the substrate. Future work could use inert surfaces that do allow sporozoites to only partially attach, which might be achieved using nanostructured substrates with defined adhesion sites[49] for dissecting the forces a sporozoite exerts on natural substrates.

Loss of Transduction Force in Motile *s6(-)* and *trap(-)* Sporozoites. Hemolymph sporozoites undergo a multistep process from floating to gliding.[20] In contrast to salivary-gland-derived parasites, hemolymph sporozoites also perform patch gliding as an additional motility type.[13] It is not clear what use this movement is to the sporozoite, and it might reflect a nonmature form of motility. In fact, sporozoites are rarely observed to convert from patch gliding to gliding, suggesting that indeed the proteins of the motility machinery are not yet expressed or not yet perfectly assembled in patch gliding sporozoites. Nevertheless, during patch gliding, sporozoites move as fast as during rapid periods of continuous gliding. Thus, examining patch gliding parasites should yield information about forces occurring during gliding at a single adhesion site, something hard to observe during gliding of mature sporozoites, where multiple adhesions are rapidly formed and turned over.[13] Attempts to trap a patch gliding WT sporozoite with 6.6 ± 1.4 pN trapping force were not successful and did not even slow down the sporozoite. This indicates that the motor machinery is effectively working by applying forces far stronger than 6.6 pN. If we consider that during patch gliding a sporozoite is attached to the substratum with an area of its membrane of at least 300 nm by 300 nm,[13,38] this should leave enough space for several dozen small actin filaments.[24,25] Considering further that several myosin's can bind to and exert force on these filaments with a single myosin producing around 1−5 pN of force,[50−52] it is not surprising that we could not trap these parasites with just 6.6 ± 1.4 pN of counterforce. This also indicates that the order of just 10 myosins might be sufficient for force production at any moment to propel the sporozoite. Interestingly, patch gliding *trap(-)* as well as *s6(-)* sporozoites were easily trapped at a trapping force of 6.6 ± 1.4 pN. This indicates important roles for both TRAP and S6 in either

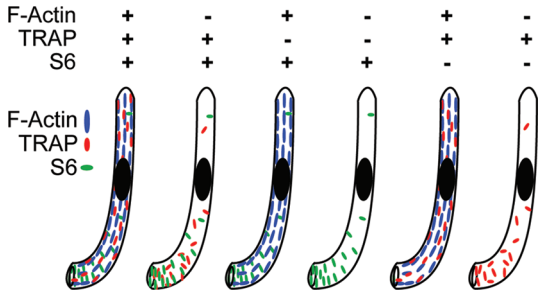

Figure 7. Cartoon illustrating the proposed functional distribution of actin filaments (blue), TRAP (red), and S6 (green) in the different experimental settings as indicated on top. We propose that TRAP but not S6 is distributed along the sporozoite surface by actin filaments. In sporozoites incubated with cytochalasin D (absence of F-actin), no actin filaments are visible and both TRAP and S6 accumulate at the tip (bottom) of the sporozoite. Note that S6 is drawn perpendicular and TRAP parallel to the sporozoite axis. These denote the functional differences in linear and lateral cohesion that we observed in the respective mutants and which are reported in Figure 5. Also note that the proposed functional localization might not completely reflect the localization of the respective proteins on the sporozoite surface.

generating actin filaments needed for myosin force production and/or in transducing the generated forces to the substrate.

Differences in Primary Adhesion between *trap(-)* and *s6(-)* Sporozoites. For effective sporozoite motility, motor function and adhesion turnover are important. Hemolymph sporozoites allow us to distinguish between the motor and adhesion machinery: Patch gliding parasites possess an already functioning force-creating motor machinery on one hand. On the other hand, the mechanisms for adhesion formation and turnover are not yet fully developed, resulting in an incomplete and thus ineffective interplay between the respective sets of proteins.

While *trap(-)* and *s6(-)* sporozoites undergoing patch gliding could be trapped, neither parasites could be ripped off the substrate once one adhesion site was formed. This suggests little, if any, contribution of S6 and TRAP to the adhesion strength, although the optical tweezers might be too weak to reveal quantitative differences of this effect.

Indeed, only a small fraction of *trap(-)* and *s6(-)* sporozoites do adhere by themselves,[20] suggesting that both proteins are required for the formation of a first adhesion site but are dispensable once this adhesion has been formed. Alternatively, or in addition to their effect in adhesion, they might be involved in promoting de-adhesion, probably along with actin filaments. In this way, their absence would lead to reduced de-adhesion upon adhesion establishment. Indeed, this is what was found previously for *trap(-)* sporozoites.[13]

Curiously, there was a striking difference in the orientation with which *trap(-)* and *s6(-)* sporozoites attached to a surface. Floating sporozoites show no active swimming movement. Thus we assume that the probability to touch a substrate with a given surface area relies solely on the geometry of a passively floating object. The shape of hemolymph sporozoites resembles a "J",[6] indicating a high, yet not perfect, morphological symmetry. If the surface of sporozoites possesses an equally and evenly distributed adhesiveness, a random distribution for the occurrence of the initial adhesion would be expected. However, *trap(-)* sporozoites in the absence or presence of cytochalasin D as well as wild-type and *s6(-)* sporozoites in the presence of cytochalasin D adhered mostly (around 75% of observed sporozoites) with their apical pole. Only *s6(-)* sporozoites showed no such preferential adhesion along their cell body (Figure 4B).

TABLE 1. Semiquantitative Summary of the Effects of Actin Filaments, TRAP, or S6 by Themselves or in the Indicated Combinations on Polarized Adhesion and Cohesion of the First Adhesion Site[a]

	polarized adhesion[b]	lateral cohesion[c]	linear cohesion at front[d]	linear cohesion at rear[d]
actin filaments	0	0	0	n.d.
TRAP	0	+	0	+
S6	++	0	++	0
TRAP/F-actin	0	+	0	++
S6/F-actin	0	0	0	0

[a] As we cannot compare to wild-type, the baseline is set for the WT/F-actin(-) parasite or similar phenotypes of WT/F-actin(-) and *trap(-)* parasites; 0 represents no effect, + possible positive effect ($p < 0.1$), and ++ statistically significant positive effect ($p < 0.05$). [b] See Figures 4 and 6. [c] See Figure S2. [d] See Figure 5 (rear stands for rear and central); n.d.: not determinable from the data at hand as cytochalasin D affects linear cohesion at rear for TRAP but not S6 parasites. Wild-type parasites could not be probed in the absence of cytochalasin D. See also Figure S3 for a complementary list.

TRAP and S6 are secreted to the plasma membrane by the fusion of micronemal vesicles at the sporozoite front. Both proteins are thought to be transported in an actin-dependent fashion toward the rear on the plasma membrane.[12] This could lead to a high concentration of both proteins at the front end, especially in the absence of actin filaments, when most secreted micronemal proteins could remain at the apical end, thus making it more adhesive compared to the rest of the sporozoite.

Our results suggest a functional asymmetry regarding the distribution of adhesive molecules. Unfortunately, the inaccessibility of wild-type sporozoites for our functional assays makes interpretation somewhat ambiguous. Nevertheless, with several conditions giving similar and others distinct results, we suggest the following: S6 might be localized and/or induces adhesion at the front end and shows little impact on adhesion events at the rear end of sporozoites (Figure 5C, Figure 7, Table 1). Furthermore, we suggest TRAP to be evenly distributed along the sporozoites *via* dynamic actin filaments. The absence of actin filaments

results in an asymmetric spreading of TRAP going along with a pronounced adhesiveness at the front (Figure 7). Consequently, S6 in coordination with F-actin but not TRAP or actin filaments alone appears responsible for the strong polarization of adhesion toward the front end. Curiously, previous localization studies on sporozoites showed a punctuate pattern for S6[21] and a uniform or punctate localization for TRAP.[53,54] Thus, a combination of functional assays with live-cell surface-sensitive imaging of sporozoites expressing fluorescently labeled functional S6 and TRAP will be needed to shed more light on their function during adhesion formation.

Actin Filaments and Lateral Cohesion. The effectiveness of a cell binding to a substrate is determined by the strength of the adhesion site as mediated by the binding of adhesins to substrate molecules as well as by the molecular cohesion within the substrate binding area of the cells as mediated by the interaction of cellular molecules among themselves. Cohesion could depend on the lipid composition of the plasma membrane as well as homogeneous or heterogeneous interactions between adhesins or the interactions between adhesins and the cytoskeleton. To probe cohesion of a substrate binding area, we used rotatability and the potential to pull a sporozoite over its initial adhesion site as different measures for lateral and linear cohesion, respectively (Figures 3, 5 and S2).

Sporozoites can show a cytochalasin D sensitive waving motion, indicating a currently unclear F-actin-based movement mechanism.[20] The current model of the motility machinery[11] suggests an orientation for F-actin in the apical posterior direction. Provided that the motility machinery is also present at the initial adhesion site, actin filaments that are oriented in an apical posterior way could induce strong lateral cohesion and thus limit the ability to rotate the sporozoite. However, when we compared the rotatabilty of sporozoites using laser tweezers, we found no significant difference between cytochalasin D treated and untreated sporozoites. This result indicates that F-actin (a) may not be present at the primary adhesion patch, (b) is too weak to lead to a measurable effect, (c) is not strictly oriented in apical posterior direction, or (d) plays no role in counteracting the rotational movement. Unfortunately, even high-resolution visualization techniques such as electron microscopy so far failed to visualize apicomplexan actin filaments,[24,26,55] leaving a final interpretation regarding the role of F-actin in lateral cohesion unclear.

Different Roles of TRAP and S6 in Parasite Adhesion and Motility. S6 is important for linear cohesion but appears to play no role in lateral cohesion. In contrast, TRAP might play a weak role in restricting rotatability (p = 0.07) but has no role in linear cohesion (Figure S2). These observations suggest that both TRAP and S6 are involved in mediating structural stiffness within a single adhesion site with their direction of action possibly being orthogonal to one another (Figures 7 and 8). Using traction force microscopy, different parts of the parasite appeared to produce forces in different directions.[13] At the tip of the parasite, traction force vectors pointed toward the center of the parasite, that is, along its longitudinal axis. At the center of the parasite, they pointed orthogonally toward the cell center. Also, *trap(-)* sporozoites do not show circular gliding at all but still undergo patch gliding.[10,13] In combination with the results presented in this paper, we propose that orthogonal traction forces are not necessary for linear patch gliding but essential for circular (forward) gliding. TRAP might be involved in the generation of traction forces in the orthogonal direction, thus making efficient gliding possible.

Similar proportions of all tested sporozoites underwent patch gliding in the absence of cytochalasin D. Surprisingly in the presence of cytochalasin D (*i.e.*, absence of actin filaments), WT sporozoites could rarely be pulled over an initial adhesion site (Figure 5B). This suggests that actin actively lowers the cohesive strength of an adhesion site. This is in line with previous observations that application of jasplakinolide, which stabilizes actin filaments and leads to more F-actin in parasites,[56] results in lower traction forces and the detachment of sporozoites.[13] In the presence of cytochalasin D, *trap(-)* sporozoites could be pulled over the initial adhesion site somewhat (p = 0.08) more often than WT sporozoites (Figure 5B), indicating a possible weak role for TRAP in linear cohesion. Strikingly, in the absence of S6, 66% of all tested sporozoites could be pulled over the adhesion site, suggesting that a main role of S6 is to mediate linear cohesion within the initial adhesion site. Treatment of *s6(-)* sporozoites with cytochalasin D massively diminished this effect, indicating again that the absence of actin filaments leads to more cohesive sporozoite adhesions. We thus propose that S6 serves as an actin-to-substrate linker and functions in strengthening the cohesion of the initial adhesion site, although we cannot directly compare it with the wild-type.

TRAP and S6 Modulate Actin-Dependent Cohesion at Different Locations. The cohesion of an adhesion site can depend on its location along the sporozoite cell body. In *s6(-)* sporozoites, there was no difference if a parasite was attached at the front, center, or rear in terms of its resistance against pulling (Figure 5C). However, after addition of cytochalasin D, only few parasites attached at the front end could still be pulled over their initial adhesion site. In contrast, those attached at the center or rear showed only a slight decrease in cohesion. In contrast, *trap(-)* sporozoites could readily be pulled over the adhesion and also showed little difference between parasites adhering at the front or at the center/rear. Intriguingly, when cytochalasin D was added, the parasites adhering at the front remained

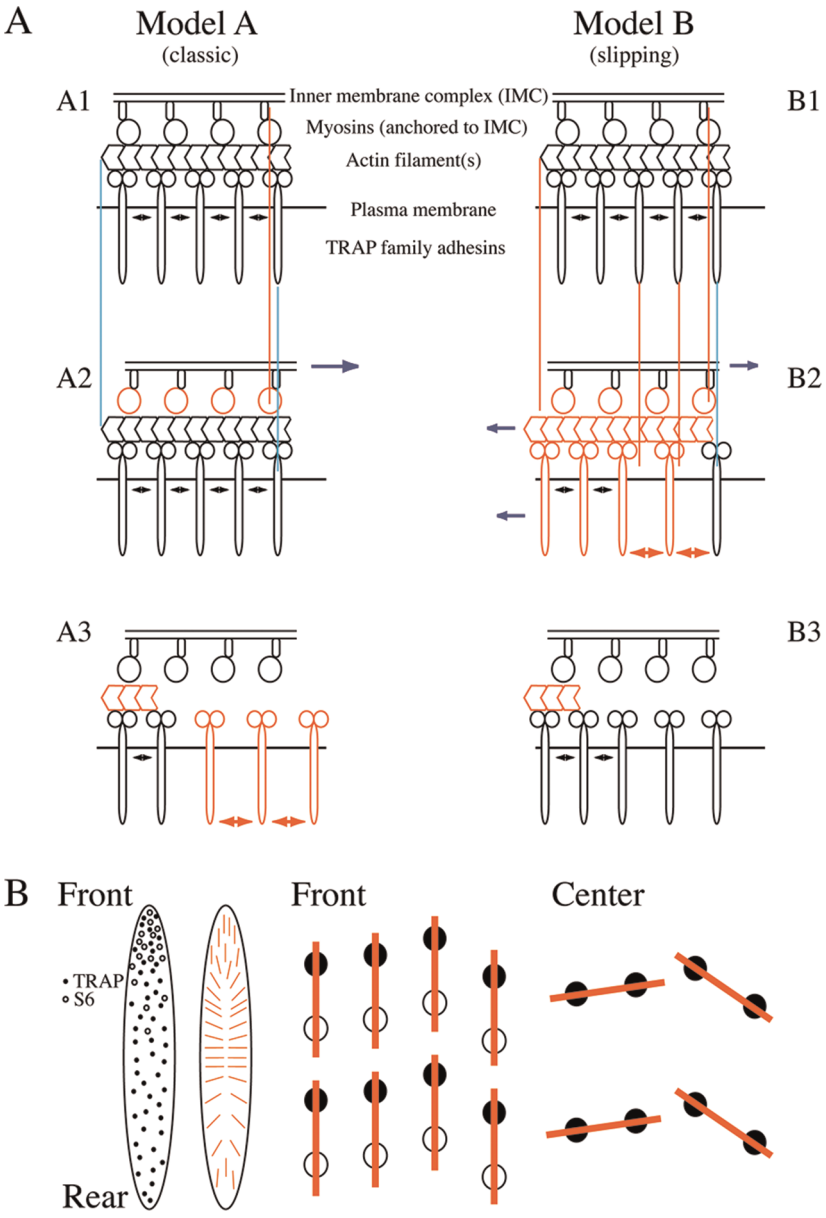

Figure 8. Cohesion of slipping adhesion sites during motility. (A) Two models of how cohesion (black double arrows) of an adhesion site could be weakened during motility. Myosin heads bind to actin filaments that in turn are linked to plasma membrane spanning adhesins *via* an aldolase complex. The adhesins in turn bind to the substrate (not shown). Red objects and lines indicate changes to the previous panel; cyan lines indicate objects that do not change. In the classic model describing apicomplexan motility (model A), the myosin powerstroke leads to a displacement of the myosins anchored to the inner membrane complex (IMC) as indicated by the blue arrow in A2, while the adhesins and actin filaments stay put in respect to the substrate. Loss of cohesion could occur in this model after depolymerization of actin (A3) when the adhesins could diffuse in the plasma membrane (red double arrows). This model would suggest less cohesion to occur under cytochalasin D (no more actin filaments). We observed this for the *trap(-)* sporozoites at the center and rear. In a model more likely to describe the slipping adhesions of the sporozoite (model B), the myosin powerstroke leads to a displacement of the myosins anchored to the IMC but also to a displacement in opposite direction of the actin filament and the adhesins (B2, blue arrows). Loss of cohesion thus could occur by actin filament displacement. This model would suggest that cohesion stays the same under cytochalasin D. We observed this for the *trap(-)* sporozoites at the front (strong cohesion) and the *s6(-)* sporozoites at center and rear (weak cohesion). (B) Highly speculative model of the functional distribution of TRAP and S6 along the sporozoite and how some of the observed differences in linear and lateral cohesion could be based on differently arranged actin filaments (red bars, not to scale for better visualization). At the front, both TRAP and S6 might interact with actin filaments, leading to a linear array ideal for forward movement. Absence of S6 would lead to an arrangement of filaments on the front as it would normally occur at the center, where only TRAP would interact with filaments, which are less ordered, thus leading to resistance against a linear force. Such filament arrangements could also possibly lead to the lateral traction forces exerted onto the substrate as described in Münter *et al.*, 2009.

adverse to pulling, while almost all adhering at the center or rear could readily be pulled over their first adhesion site (Figure 5C). Thus, while depolymerization of actin leads to greater cohesion in *s6(-)* sporozoites, it

has no effect on *trap(-)* sporozoites adhering with their front, but it even decreases cohesion of *trap(-)* sporozoites attached at the center or rear of the parasite (Figure 5C). As for the following adhesion steps, in our experimental setup, neither actin filaments, nor S6, nor TRAP appeared to play a major role in the formation of the second adhesion (Figure 6C). This does not formally exclude a role for these proteins in bringing the free end of a sporozoite closer to the substrate or by acting together in a way that just one missing factor would lead to failure of adhesion site formation. Alternatively, other proteins on the sporozoite surface might mediate formation of the second adhesion site. The *s6(-)* sporozoites showed a significantly higher success rate for secondary adhesion formation in our experiments. This was likely due to their decreased cohesion of the first adhesion site, which thus allowed *s6(-)* sporozoites to use their adhesive apical end for formation of the second adhesion side.

CONCLUSION

Taken together (Table 1, Figures 7 and 8), these observations constitute the first descriptions of a spatially segregated functional effect of proteins on the *Plasmodium* sporozoite surface. Our data suggest that S6 somehow interferes with TRAP–actin interactions in order to generate forward movement and that actin filaments distribute TRAP but not necessarily S6. Thus, it is tempting to speculate how the interaction of the two TRAP family adhesins with actin filaments is regulated. One possibility would be that a different affinity of the cytoplasmic tails of S6 and TRAP for aldolase, which links TRAP family adhesins to actin filaments,[57] causes different cohesive strength, for example, by the generation of different filament assemblies under the plasma membrane. Alternatively, it might be possible that the different extracellular domains of the two adhesins convey different signals. These possibilities could be tested by domain-swap experiments, for example, by generation of recombinant parasites that express chimeras of S6 and TRAP instead of the respective adhesin. Importantly, laser tweezers, together with the recently published toolset of tunable substrates,[58] can now be used to dissect the process of parasite adhesion and motility with previously unimagined precision.

METHODS

Ethics Statement. All animal experiments were performed concerning FELASA category B and GV-SOLAS standard guidelines. Animal experiments were approved by German authorities (Regierungspräsidium Karlsruhe, Germany), § 8 Abs. 1 Tierschutzgesetz (TierSchG).

Animals. *Anopheles stephensi* mosquitoes were reared and infected with *Plasmodium berghei* sporozoites as described previously.[59] Briefly, NMRI mice infected with (i) wild-type *Plasmodium berghei* strains NK65 or ANKA parasites or *P. berghei* NK65 parasites expressing the green fluorescent protein under the sporozoite stage specific CS promoter,[60] (ii) *P. berghei* strain NK65 parasites lacking TRAP,[10] or (iii) *P. berghei* strain ANKA parasites lacking S6[21] were anesthetized and fed to *A. stephensi* mosquitoes 3–5 days post-hatching. So far, we failed to detect any difference in adhesion or motility between *P. berghei* strain NK65 and ANKA sporozoites and thus used them interchangeably. Mosquitoes were then kept in dedicated incubators at 21 °C and >70% humidity until dissected for experimentation. Hemolymph sporozoites were dissected by rinsing infected mosquito hemolymph with 5–10 μL of RPMI tissue culture medium containing 3% bovine serum albumin, if not stated differently. Sporozoites were kept on ice for up to 4 h before being used.

Laser Trap Setup. Laser trapping experiments with sporozoites were performed on a combined optical tweezers and fluorescence microscopy setup based on an Alpha SNOM platform (Witec) which has been described previously[61] (Figure S1). In short, a 5 W Nd:VO_4 laser (1064 nm, J20-BL-106C; Spectra Physics) collimated by a 63× water immersion objective (NA 1.2, Olympus) was used for trapping of sporozoites. Fluorescence excitation was provided by a diode laser (at 532 nm, 50 mW, Roithner Lasertechnik). Images were detected with three cameras (Retiga EX, Qimaging; Phantom v7.3, Vision Research and AxioCam, Zeiss).

Sample Preparation and Imaging. Laser trap experiments were conducted in homemade microscopy chambers consisting of two coverslips, spaced by double-sided sticky tape. Into the tape, a chamber measuring about 5 × 5 mm was cut as reservoir. Dissected sporozoites were kept on ice and used for up to 4 h after dissection. For imaging, fresh samples were taken every 45–60 min from the chilled stock since sporozoites lose their motile activity at room temperature after 60 min.[30] Sytox Orange (Invitrogen, Karlsruhe, Germany) was employed at a concentration of 5 μM as a fluorescent marker to trace the sporozoite nucleus. At this concentration, the otherwise membrane-impermeable dye does penetrate the cell membrane at sufficient concentrations to mark the position of the nucleus. As the nucleus is located toward the rear of the parasite,[38] this allowed the determination of the orientation of the sporozoites and also served as a control for sporozoite viability. In order to depolymerize actin filaments, cytochalasin D (Merck Biosciences, Nottingham, UK) was used at concentrations of 2 μM. Typical laser power for adhesion forming experiments was 100 mW in the sample plane, based on a objective specific transmissibility of 60%. In experiments aiming at detaching sporozoites, trapping powers up to 450 mW were used. Sporozoites were trapped and manipulated in the *xy*-plane using the micrometer table and in *z*-direction using the piezo stage, controlled by labVIEW routines.

Experimental Design. Hemolymph sporozoites were allowed to attach onto a glass surface. Once sporozoites had formed a single adhesion site, they were examined for localization of the adhesion at the front end or back end using the Sytox Orange fluorescence of the nucleus. Furthermore, the fluorescence signal was used to check for the viability of the sporozoite. This was done regularly during the forthcoming experiment.

In order to measure the cohesion properties of the adhesion site, we trapped the free-floating end and attempted translocating the sporozoite over its adhesion site by using laser tweezers. We differentiated between lateral and linear cohesion:

Lateral cohesion was defined as the ability of the sporozoite to resist rotation of the free end in a circular fashion around its initial adhesion site, thus measuring the maximal rotational amplitude in angular degrees. Linear cohesion was defined as the potential of the sporozoite to resist translocation of its cell body along its apical posterior axis relative to the initial

adhesion site, without actually changing the position of the adhesion site on the glass surface. Attempts to test for linear cohesion were categorized in either successful (front and rear end swap positions relative to the adhesion patch) or not successful. Note that as a consequence of a successful attempt for probing linear cohesion a sporozoite originally adhering at the front would subsequently adhere at the back, resulting in the possibility to probe the now free front end for the formation of a secondary adhesion site. Thus, we subclassified between linear cohesion at front/rear for parasites initially adhering with either end. Subsequently, the sporozoites were trapped with the optical tweezers at the free end and pressed against the glass surface by changing the height of the laser focus relatively to the glass surface. Pulling the sporozoite onto the surface allowed us to actively induce the formation of a second adhesion at the trapped end.

Hereby, all possible sides of the sporozoite were brought into contact with the surface to probe for potential adhesive loci using the laser trap to move the free end of sporozoites in all three dimensions. If no secondary adhesion was formed within 200 s, the sporozoite was counted as not forming a secondary adhesion. Doing so, we could determine the location of the newly formed adhesion by using the orientation data from fluorescence imaging. Once an adhesion was formed, it was probed by pulling the trap upward to check for the stability of the adhesion bond.

Examination of Adhesion States. In order to determine the adhesion state of individual sporozoites, parasites were placed in an uncoated flow chamber (uncoated μ-Slide I for live cell analysis; Ibidi, Martinsried, Germany) and allowed to adhere for 10 min. Movies were obtained at 1 Hz using an Axiovert 200 (Carl Zeiss) microscope with a 10× Apoplan objective (NA 0.25) and saved as zvi (Zeiss Vision Image). Analysis was performed using ImageJ based on the following definitions: 0 adhesions, floating parasites; 1 adhesion, sporozoites with one end attached to the glass surface and the other end either actively (waving) or passively (attached) moving in the medium; 2 adhesions, parasites with two adhesion points (either at both ends or at the middle as well as at any end) and a clearly distinguishable unattached area; 3 adhesions, gliding sporozoites as well as not moving, however, entirely adhered parasites.

Every sporozoite was observed for 100 s. Only the maximal adhesion state was counted in order to avoid double counting.

Data Analysis. All movies were kept in original multi-tif format, processed using Adobe After Effects and exported as AVI for analysis in ImageJ (http://rsbweb.nih.gov/ij/) or FIJI (http://pacific.mpi-cbg.de/wiki/index.php/Fiji). Statistical analyses on categorized data were performed using Fisher's exact test, which is a specialization of the χ-square test and applies to small sample sizes. Fisher's exact test was performed using a 2 × 2 contingency table.[62]

Rotational data were analyzed using the Wilcoxon signed-rank test as the related samples cannot be assumed to be normally distributed. Mutant subpopulations of the same genotype were pooled since they showed no differences ($p = 0.7$).

Conflict of Interest: The authors declare no competing financial interest.

Acknowledgment. We thank Diana Scheppan and Iris Arnold for mosquito infection, Yvonne Maier and Jan-Peter Röderer for help with image analysis, Rainer Kurre for the experimental setup, Ulrich Schwarz, Mirko Singer, and Christian Boehm for discussions and comments on the manuscript.

Supporting Information Available: Additional figures and calculation of Stokes friction forces. This material is available free of charge *via* the Internet at http://pubs.acs.org.

REFERENCES AND NOTES

1. Medalia, O.; Geiger, B. Frontiers of Microscopy-Based Research into Cell-Matrix Adhesions. *Curr. Opin. Cell Biol.* **2010**, *22*, 659–668.
2. Boettiger, D. Quantitative Measurements of Integrin-Mediated Adhesion to Extracellular Matrix. *Methods Enzymol.* **2007**, *426*, 1–25.
3. Wehrle-Haller, B.; Imhof, B. A. Actin, Microtubules and Focal Adhesion Dynamics during Cell Migration. *Int. J. Biochem. Cell Biol.* **2003**, *35*, 39–50.
4. Munevar, S.; Wang, Y. L.; Dembo, M. Distinct Roles of Frontal and Rear Cell-Substrate Adhesions in Fibroblast Migration. *Mol. Biol. Cell* **2001**, *12*, 3947–3954.
5. Sidjanski, S.; Mathews, G. V.; Vanderberg, J. P. Electrophoretic Separation and Identification of Phenoloxidases in Hemolymph and Midgut of Adult *Anopheles stephensi* Mosquitoes. *J. Parasitol.* **1997**, *83*, 686–691.
6. Vanderberg, J. P. Studies on the Motility of Plasmodium Sporozoites. *J. Protozool.* **1974**, *21*, 527–537.
7. Amino, R.; Thiberge, S.; Martin, B.; Celli, S.; Shorte, S.; Frischknecht, F.; Menard, R. Quantitative Imaging of Plasmodium Transmission from Mosquito to Mammal. *Nat. Med.* **2006**, *12*, 220–224.
8. Vaughan, A. M.; Aly, A. S.; Kappe, S. H. Malaria Parasite Preerythrocytic Stage Infection: Gliding and Hiding. *Cell Host Microbe* **2008**, *4*, 209–218.
9. Ejigiri, I.; Sinnis, P. Plasmodium Sporozoite−Host Interactions from the Dermis to the Hepatocyte. *Curr. Opin. Microbiol.* **2009**, *12*, 401–407.
10. Sultan, A. A.; Thathy, V.; Frevert, U.; Robson, K. J.; Crisanti, A.; Nussenzweig, V.; Nussenzweig, R. S.; Menard, R. TRAP Is Necessary for Gliding Motility and Infectivity of Plasmodium Sporozoites. *Cell* **1997**, *90*, 511–522.
11. Baum, J.; Gilberger, T. W.; Frischknecht, F.; Meissner, M. Host−Cell Invasion by Malaria Parasites: Insights from Plasmodium and Toxoplasma. *Trends Parasitol.* **2008**, *24*, 557–563.
12. Morahan, B. J.; Wang, L.; Coppel, R. L. No TRAP, No Invasion. *Trends Parasitol.* **2009**, *25*, 77–84.
13. Munter, S.; Sabass, B.; Selhuber-Unkel, C.; Kudryashev, M.; Hegge, S.; Engel, U.; Spatz, J. P.; Matuschewski, K.; Schwarz, U. S.; Frischknecht, F. Plasmodium Sporozoite Motility Is Modulated by the Turnover of Discrete Adhesion Sites. *Cell Host Microbe* **2009**, *6*, 551–562.
14. Simonetti, A. B.; Billingsley, P. F.; Winger, L. A.; Sinden, R. E. Kinetics of Expression of Two Major *Plasmodium berghei* Antigens in the Mosquito Vector, *Anopheles stephensi*. *J. Eukaryotic Microbiol.* **1993**, *40*, 569–576.
15. Aly, A. S.; Vaughan, A. M.; Kappe, S. H. Malaria Parasite Development in the Mosquito and Infection of the Mammalian Host. *Annu. Rev. Microbiol.* **2009**, *63*, 195–221.
16. Kariu, T.; Yuda, M.; Yano, K.; Chinzei, Y. MAEBL Is Essential for Malarial Sporozoite Infection of the Mosquito Salivary Gland. *J. Exp. Med.* **2002**, *195*, 1317–1323.
17. Thompson, J.; Fernandez-Reyes, D.; Sharling, L.; Moore, S. G.; Eling, W. M.; Kyes, S. A.; Newbold, C. I.; Kafatos, F. C.; Janse, C. J.; Waters, A. P. Plasmodium Cysteine Repeat Modular Proteins 1−4: Complex Proteins with Roles Throughout the Malaria Parasite Life Cycle. *Cell. Microbiol.* **2007**, *9*, 1466–1480.
18. Lepper, S.; Merkel, M.; Sartori, A.; Cyrklaff, M.; Frischknecht, F. Rapid Quantification of the Effects of Blotting for Correlation of Light and Cryo-Light Microscopy Images. *J. Microsc.* **2010**, *238*, 21–26.
19. Hellmann, J. K.; Münter, S.; Kudryashev, M.; Schulz, S.; Heiss, K.; Müller, A.-K.; Matuschewski, K.; Spatz, J. P.; Schwarz, U. S.; Frischknecht, F. Environmental Constraints Guide Migration of Malaria Parasites during Transmission. *PLoS Pathog.* **2011**, *7*, e1002080.
20. Hegge, S.; Munter, S.; Steinbuchel, M.; Heiss, K.; Engel, U.; Matuschewski, K.; Frischknecht, F. Multistep Adhesion of Plasmodium Sporozoites. *FASEB J.* **2010**, *24*, 2222–2234.
21. Steinbuechel, M.; Matuschewski, K. Role for the Plasmodium Sporozoite-Specific Transmembrane Protein S6 in Parasite Motility and Efficient Malaria Transmission. *Cell. Microbiol.* **2009**, *11*, 279–288.
22. Heiss, K.; Nie, H.; Kumar, S.; Daly, T. M.; Bergman, L. W.; Matuschewski, K. Functional Characterization of a Redundant Plasmodium TRAP Family Invasin, TRAP-like Protein,

by Aldolase Binding and a Genetic Complementation Test. *Eukaryotic Cell* **2008**, *7*, 1062–1070.
23. Schuler, H.; Mueller, A. K.; Matuschewski, K. Unusual Properties of Plasmodium Falciparum Actin: New Insights into Microfilament Dynamics of Apicomplexan Parasites. *FEBS Lett.* **2005**, *579*, 655–660.
24. Sahoo, N.; Beatty, W.; Heuser, J.; Sept, D.; Sibley, L. D. Unusual Kinetic and Structural Properties Control Rapid Assembly and Turnover of Actin in the Parasite Toxoplasma Gondii. *Mol. Biol. Cell* **2006**, *17*, 895–906.
25. Schmitz, S.; Grainger, M.; Howell, S.; Calder, L. J.; Gaeb, M.; Pinder, J. C.; Holder, A. A.; Veigel, C. Malaria Parasite Actin Filaments Are Very Short. *J. Mol. Biol.* **2005**, *349*, 113–125.
26. Kudryashev, M.; Lepper, S.; Baumeister, W.; Cyrklaff, M.; Frischknecht, F. Geometric Constrains for Detecting Short Actin Filaments by Cryogenic Electron Tomography. *PMC Biophys.* **2010**, *3*, 6.
27. Ashkin, A.; Dziedzic, J. M.; Yamane, T. Optical Trapping and Manipulation of Single Cells Using Infrared Laser Beams. *Nature* **1987**, *330*, 769–771.
28. Suresh, S.; Spatz, J.; Mills, J. P.; Micoulet, A.; Dao, M.; Lim, C. T.; Beil, M.; Seufferlein, T. Connections between Single-Cell Biomechanics and Human Disease States: Gastrointestinal Cancer and Malaria. *Acta Biomater.* **2005**, *1*, 15–30.
29. Mills, J. P.; Diez-Silva, M.; Quinn, D. J.; Dao, M.; Lang, M. J.; Tan, K. S.; Lim, C. T.; Milon, G.; David, P. H.; Mercereau-Puijalon, O.; Bonnefoy, S.; Suresh, S. Effect of Plasmodial RESA Protein on Deformability of Human Red Blood Cells Harboring Plasmodium Falciparum. *Proc. Natl. Acad. Sci. U.S.A.* **2007**, *104*, 9213–9217.
30. Hegge, S.; Kudryashev, M.; Smith, A.; Frischknecht, F. Automated Classification of Plasmodium Sporozoite Movement Patterns Reveals a Shift towards Productive Motility during Salivary Gland Infection. *Biotechnol. J.* **2009**, *4*, 903–913.
31. Liu, Y.; Sonek, G. J.; Berns, M. W.; Tromberg, B. J. Physiological Monitoring of Optically Trapped Cells: Assessing the Effects of Confinement by 1064-nm Laser Tweezers Using Microfluorometry. *Biophys. J.* **1996**, *71*, 2158–2167.
32. Neuman, K. C.; Chadd, E. H.; Liou, G. F.; Bergman, K.; Block, S. M. Characterization of Photodamage to *Escherichia coli* in Optical Traps. *Biophys. J.* **1999**, *77*, 2856–2863.
33. Peterman, E. J.; Gittes, F.; Schmidt, C. F. Laser-Induced Heating in Optical Traps. *Biophys. J.* **2003**, *84*, 1308–1316.
34. Svoboda, K.; Block, S. M. Biological Applications of Optical Forces. *Annu. Rev. Biophys. Biomol. Struct.* **1994**, *23*, 247–285.
35. Neuman, K. C.; Block, S. M. Optical Trapping. *Rev. Sci. Instrum.* **2004**, *75*, 2787–2809.
36. Thoumine, O.; Kocian, P.; Kottelat, A.; Meister, J. J. Short-Term Binding of Fibroblasts to Fibronectin: Optical Tweezers Experiments and Probabilistic Analysis. *Eur. Biophys. J.* **2000**, *29*, 398–408.
37. Vanderberg, J. P.; Rdodin, J.; Yoeli, R. Electron Microscopic and Histochemical Studies of Sporozoite Formation in Plasmodium Berghei. *J. Eukaryotic Microbiol.* **1967**, *14*, 82–103.
38. Kudryashev, M.; Lepper, S.; Stanway, R.; Bohn, S.; Baumeister, W.; Cyrklaff, M.; Frischknecht, F. Positioning of Large Organelles by a Membrane-Associated Cytoskeleton in Plasmodium Sporozoites. *Cell. Microbiol.* **2010**, *12*, 362–371.
39. Coppi, A.; Tewari, R.; Bishop, J. R.; Bennett, B. L.; Lawrence, R.; Esko, J. D.; Billker, O.; Sinnis, P. Heparan Sulfate Proteoglycans Provide a Signal to Plasmodium Sporozoites To Stop Migrating and Productively Invade Host Cells. *Cell Host Microbe* **2007**, *2*, 316–327.
40. Pradel, G.; Garapaty, S.; Frevert, U. Proteoglycans Mediate Malaria Sporozoite Targeting to the Liver. *Mol. Microbiol.* **2002**, *45*, 637–651.
41. Rathore, D.; Sacci, J. B.; de la Vega, P.; McCutchan, T. F. Binding and Invasion of Liver Cells by Plasmodium Falciparum Sporozoites. Essential Involvement of the Amino Terminus of Circumsporozoite Protein. *J. Biol. Chem.* **2002**, *277*, 7092–7098.
42. Coppi, A.; Natarajan, R.; Pradel, G.; Bennett, B. L.; James, E. R.; Roggero, M. A.; Corradin, G.; Persson, C.; Tewari, R.; Sinnis, P. The Malaria Circumsporozoite Protein Has Two Functional Domains, Each with Distinct Roles as Sporozoites Journey from Mosquito to Mammalian Host. *J. Exp. Med.* **2011**, *208*, 341–356.
43. Neuman, K. C.; Nagy, A. Single-Molecule Force Spectroscopy: Optical Tweezers, Magnetic Tweezers and Atomic Force Microscopy. *Nat. Methods* **2008**, *5*, 491–505.
44. Zhang, H.; Liu, K. K. Optical Tweezers for Single Cells. *J. R. Soc. Interface* **2008**, *5*, 671–690.
45. Pozzo, L. Y.; Fontes, A.; de Thomaz, A. A.; Santos, B. S.; Farias, P. M.; Ayres, D. C.; Giorgio, S.; Cesar, C. L. Studying Taxis in Real Time Using Optical Tweezers: Applications for *Leishmania amazonensis* Parasites. *Micron* **2009**, *40*, 617–620.
46. Krasnikov, I.; Seteikin, A.; Bernhardt, I. Thermal Processes in Red Blood Cells Exposed to Infrared Laser Tweezers (λ = 1064 nm). *J. Biophotonics* **2011**, *4*, 206–212.
47. Kress, H.; Stelzer, E. H.; Holzer, D.; Buss, F.; Griffiths, G.; Rohrbach, A. Filopodia Act as Phagocytic Tentacles and Pull with Discrete Steps and a Load-Dependent Velocity. *Proc. Natl. Acad. Sci. U.S.A.* **2007**, *104*, 11633–11638.
48. Florin, E. L.; Moy, V. T.; Gaub, H. E. Adhesion Forces between Individual Ligand-Receptor Pairs. *Science* **1994**, *264*, 415–417.
49. Spatz, J. P.; Geiger, B. Molecular Engineering of Cellular Environments: Cell Adhesion to Nano-Digital Surfaces. *Methods Cell Biol.* **2007**, *83*, 89–111.
50. Finer, J. T.; Simmons, R. M.; Spudich, J. A. Single Myosin Molecule Mechanics: Piconewton Forces and Nanometre Steps. *Nature* **1994**, *368*, 113–119.
51. Molloy, J. E.; Burns, J. E.; Kendrick-Jones, J.; Tregear, R. T.; White, D. C. Movement and Force Produced by a Single Myosin Head. *Nature* **1995**, *378*, 209–212.
52. Nishizaka, T.; Miyata, H.; Yoshikawa, H.; Ishiwata, S.; Kinosita, K., Jr. Unbinding Force of a Single Motor Molecule of Muscle Measured Using Optical Tweezers. *Nature* **1995**, *377*, 251–254.
53. Gantt, S.; Persson, C.; Rose, K.; Birkett, A. J.; Abagyan, R.; Nussenzweig, V. Antibodies Against Thrombospondin-Related Anonymous Protein Do Not Inhibit Plasmodium Sporozoite Infectivity *in Vivo*. *Infect. Immun.* **2000**, *68*, 3667–3673.
54. Rennenberg, A.; Lehmann, C.; Heitmann, A.; Witt, T.; Hansen, G.; Nagarajan, K.; Deschermeier, C.; Turk, V.; Hilgenfeld, R.; Heussler, V. T. Exoerythrocytic Plasmodium Parasites Secrete a Cysteine Protease Inhibitor Involved in Sporozoite Invasion and Capable of Blocking Cell Death of Host Hepatocytes. *PLoS Pathog.* **2010**, *6*, e1000825.
55. Wetzel, D. M.; Hakansson, S.; Hu, K.; Roos, D.; Sibley, L. D. Actin Filament Polymerization Regulates Gliding Motility by Apicomplexan Parasites. *Mol. Biol. Cell* **2003**, *14*, 396–406.
56. Wetzel, D. M.; Chen, L. A.; Ruiz, F. A.; Moreno, S. N.; Sibley, L. D. Calcium-Mediated Protein Secretion Potentiates Motility in *Toxoplasma gondii*. *J. Cell Sci.* **2004**, *117*, 5739–5748.
57. Starnes, G. L.; Coincon, M.; Sygusch, J.; Sibley, L. D. Aldolase Is Essential for Energy Production and Bridging Adhesin-Actin Cytoskeletal Interactions during Parasite Invasion of Host Cells. *Cell Host Microbe* **2009**, *5*, 353–64.
58. Perschmann, N.; Hellmann, J. K.; Frischknecht, F.; Spatz, J. P. Induction of Malaria Parasite Migration by Synthetically Tunable Microenvironments. *Nano Lett.* **2011**, *11*, 4468–4474.
59. Hellmann, J. K.; Munter, S.; Wink, M.; Frischknecht, F. Synergistic and Additive Effects of Epigallocatechin Gallate and Digitonin on Plasmodium Sporozoite Survival and Motility. *PLoS One* **2010**, *5*, e8682.
60. Natarajan, R.; Thathy, V.; Mota, M. M.; Hafalla, J. C.; Menard, R.; Vernick, K. D. Fluorescent Plasmodium Berghei Sporozoites and Pre-erythrocytic Stages: A New Tool To Study Mosquito and Mammalian Host Interactions with Malaria Parasites. *Cell. Microbiol.* **2001**, *3*, 371–379.

61. Uhrig, K.; Kurre, R.; Schmitz, C.; Curtis, J. E.; Haraszti, T.; Clemen, A. E.; Spatz, J. P. Optical Force Sensor Array in a Microfluidic Device Based on Holographic Optical Tweezers. *Lab Chip* **2009**, *9*, 661–668.
62. Agresti, A. A Survey of Exact Interference for Contingency Tables. *Stat. Sci.* **1992**, *7*, 131–137.